DOI: 10.1002/chem.200801659

Vacuum-UV Irradiation-Based Formation of Methyl-Si-O-Si Networks from Poly(1,1-Dimethylsilazane-*co*-1-methylsilazane)

Lutz Prager,*[a] Luise Wennrich,[a] Roswitha Heller,[a] Wolfgang Knolle,[a] Sergej Naumov,[a] Andrea Prager,[a] Daniel Decker,[b] Hubert Liebe,[b] and Michael R. Buchmeiser*[a, c]

Abstract: The vacuum-UV (VUV)-induced conversion of commercially available poly(1,1-dimethylsilazane-*co*-1-methylsilazane) into methyl-Si-O-Si networks was studied using UV sources at wavelengths around 172, 185, and 222 nm, respectively. Time-of-flight secondary ion mass spectroscopy (TOF-SIMS), X-ray photo electron spectroscopy (XPS), and Fourier transform infrared (FTIR) measurements, as well as kinetic investigations, were carried out to elucidate the degradation process. First-order kinetics were found for the photolytically induced decomposition of the Si–NH-Si network, the subsequent formation of the methyl-Si-O-Si network and the concomitant degradation of the $Si–CH_3$ bond, which were additionally independent of the photon energy above a threshold of about 5.5 eV (225 nm). The kinetics of these processes were, however, dependent on the dose actually absorbed by the layer and, in the case of Si-O-Si formation, additionally on the oxygen concentration. The release of ammonia and methane accompanied the conversion process. Quantum-chemical calculations on methyl substituted cyclotetrasilazanes as model compounds substantiate the suggested reaction scheme. Layers <100 nm in thickness based on mixtures of poly(1,1-dimethylsilazane-*co*-1-methylsilazane) and perhydropolysilazane (PHPS) were coated onto polyethylene terephthalate (PET) foils by a continuous roll to roll process and cured by VUV irradiation by using wavelengths <200 nm and investigated for their O_2 and water vapor-barrier properties. It was found that the resulting layers displayed oxygen and water vapor transmission rates (OTR and WVTR, respectively) of $<1\,cm^3\,m^{-2}\,d^{-1}\,bar^{-1}$ and $<4\,g\,m^{-2}\,d^{-1}$, respectively.

Keywords: barrier layers · photolysis · silazanes · surface chemistry · UV irradiation

Introduction

Polysilazanes are widely investigated and practically used as precursors for SiO_x gas-barrier layers in packaging industry,[1–3] for flexible solar cells,[4,5] for applications in electronics,[6] for vacuum-insulated panels,[7] and for anticorrosive protective coatings.[8,9] Especially the inorganic oligomer perhydropolysilazane (PHPS) consisting of $-SiH_2–NH-$ structural units has been reported as a precursor to dense and stable SiO_x networks.[10–14] The most common pathway for the realization of such SiO_x networks is the hydrolysis of the Si–NH bonds and the subsequent condensation of the generated silanols forming Si–O–Si bonds.[15,16] At room temperature, this process proceeds slowly. It can, however, be moderately accelerated by the use of catalysts or basic reaction atmospheres.[17,18] With the aim to avoid the slow condensation process, alternatives that use UV irradiation as the initiating step have been applied.[19–22] Employing such a technology, improved barrier properties on polymer foils, as

[a] Dr. L. Prager, Dr. L. Wennrich, R. Heller, Dr. W. Knolle, Dr. S. Naumov, A. Prager, Prof. Dr. M. R. Buchmeiser
Leibniz-Institut für Oberflächenmodifizierung e.V.
Permoserstraße 15, 04318 Leipzig (Germany)
Fax: (+49) 341-235-2524
E-mail: lutz.prager@iom-leipzig.de
michael.buchmeiser@iom-leipzig.de

[b] Dr. D. Decker, H. Liebe
Clariant Produkte GmbH
Am Unisys-Park 1
65843 Sulzbach a. T. (Germany)

[c] Prof. Dr. M. R. Buchmeiser
Institut für Technische Chemie
Universität Leipzig
Linnéstraße 3, 04103 Leipzig (Germany)

Supporting information for this article is available on the WWW under http://dx.doi.org/10.1002/chem.200801659.

characterized by lower oxygen and water vapor transmission rates (OTR and WVTR, respectively) could be achieved in a roll-to-roll process, which was also found suitable for industrial applications.[21] However, further investigation has disclosed the problem of limited water vapor barriers caused by the desired marginal thickness of the layers (<100 nm) and by defects of the coating as caused by microcracks and pinholes. Additionally, the perceptible surface roughness of the polymer substrates itself leads to defects. The hydrophilic character of the layer, as characterized by a water contact angle around 35°, was a further crucial factor. Finally, the brittleness of such formed SiO_x layers excludes applications in which the coated foil is exposed to mechanical stress.

We, therefore, anticipated that the incorporation of methyl groups into the Si-O-Si network could reduce these limitations by modifying the thermoelastic properties (elongation at breaks, stiffness) of the layer,[23] and by enhancing the water contact angle. For these purposes, a series of polyorganosilazanes was available, for example; poly(1,1-dimethylsilazane-*co*-1-methylsilazane) (P(DMS*co*MS)), and poly(1-methylsilazane-*co*-1-methyl-1-vinylsilazane) (P(MS*co*MVS); Figure 1).

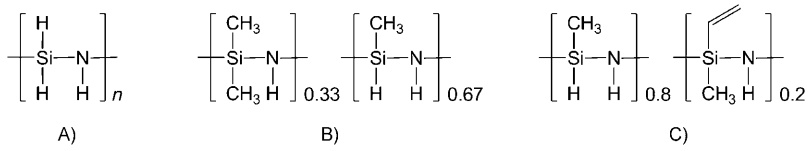

Figure 1. Structure of A) PHPS, B) P(DMS*co*MS), and C) P(MS*co*MVS).

In contrast to PHPS, the thermal curing at room temperature of both P(DMS*co*MS) and P(MS*co*MVS) was found to proceed slowly.[18] There the use of catalysts or ammonia-containing atmospheres did not result in any pronounced acceleration of the process. Based on our findings on the vacuum-ultraviolet (VUV) initiated conversion process of PHPS into SiO_x,[21] we investigated the conversion of P(DMS*co*MS) into the corresponding methyl-Si-O-Si layers using a similar approach. The main focus of this work was on the elucidation of the mechanism of the VUV-induced conversion of P(DMS*co*MS) into methyl-Si-O-Si networks with enhanced barrier properties. In addition to experiments on P(DMS*co*MS), irradiation experiments on methyl-substituted disilazanes, as model compounds, were performed, which should help in the interpretation of the results. The experimental findings were supported by quantum-chemical calculations on methyl substituted cyclotetrasilazanes as model compounds for the P(DMS*co*MS)-derived network. Based on these quantum-chemical calculations, the optical properties of thin layers of P(DMS*co*MS) and the consequences on sample design and irradiation wavelengths are discussed. TOF-SIMS and XPS measurements were carried out to monitor the depth-dependence of the chemical composition of P(DMS*co*MS)-derived alkyl-Si-O-Si layers on irradiation. Kinetic data of the conversion process of spin-coated layers under various ambient conditions based on FTIR measurements are given. These measurements further supported the mechanism of the conversion process. Finally, IR measurements of the gas phase above the irradiated P(DMS*co*MS) layers were carried out.

Results and Discussion

Quantum-chemical investigations: Recently,[21] we reported on quantum chemical calculations on the irradiation-induced oxidative conversion of PHPS into Si-O-Si networks. Parameters such as the electronic absorption spectra, energy levels of excited states, and bond dissociation energies (BDE) calculated on appropriate model molecules substantially supported the discussion of experimental results and allowed for the establishment of a reaction scheme. Similar calculations were made on cyclic organosilazanes using the DFT B3LYP method with 6-31G(d) and 6-31+G(d,p) basis sets for geometry optimization and calculation of the excitation energies, respectively, as implemented in the Gaussian 03 (Rev. B.02) package.[25] Frequency calculations were done at the same level of theory to characterize the stationary points on the potential surface and to obtain the Gibbs free energy (ΔG) at a standard temperature of 298.15 K and at a pressure of 1 atm using unscaled vibrations. Several disilazanes and cyclotetrasilazanes were chosen as model molecules for the P(DMS*co*MS) network, the latter due to their structural resemblance. As an example, the results obtained on tetramethylcyclotetrasilazane (TMCTSz) are summarized in Figure 2.

The calculation of the energy of the first excited singlet state S^1 (130 kcal mol^{-1}) showed that photons with an energy of $E > 5.6$ eV ($\lambda < 221$ nm) are required to excite the molecule. Excitation into higher singlet states S^n is likely to occur with light of $\lambda = 172$ or 185 nm, however, relaxation by fast internal conversion leads to the S^1 state, which serves as a precursor for the subsequent intersystem crossing into the excited triplet state T*. The independence of the excitation wavelength was approved by kinetic measurements (vide infra), which gave raise to virtually identical results in the range $172 < \lambda < 222$ nm. Attempts to perform a geometry optimization for the triplet state were unsuccessful. Thus, simulations starting from the excited singlet state geometry did not converge into a stable triplet conformer, instead, immediate bond elongation of a Si–NH bond was observed. The QC calculations predict that bond scission is much more likely to occur than relaxation of the excited triplet state T* into its T^1 ground state. In Figure 2, the bond dissociation energies (BDE) calculated as differences of the Gibbs free energies of the N–H, Si–NH, C–H, Si–H, and Si–CH_3

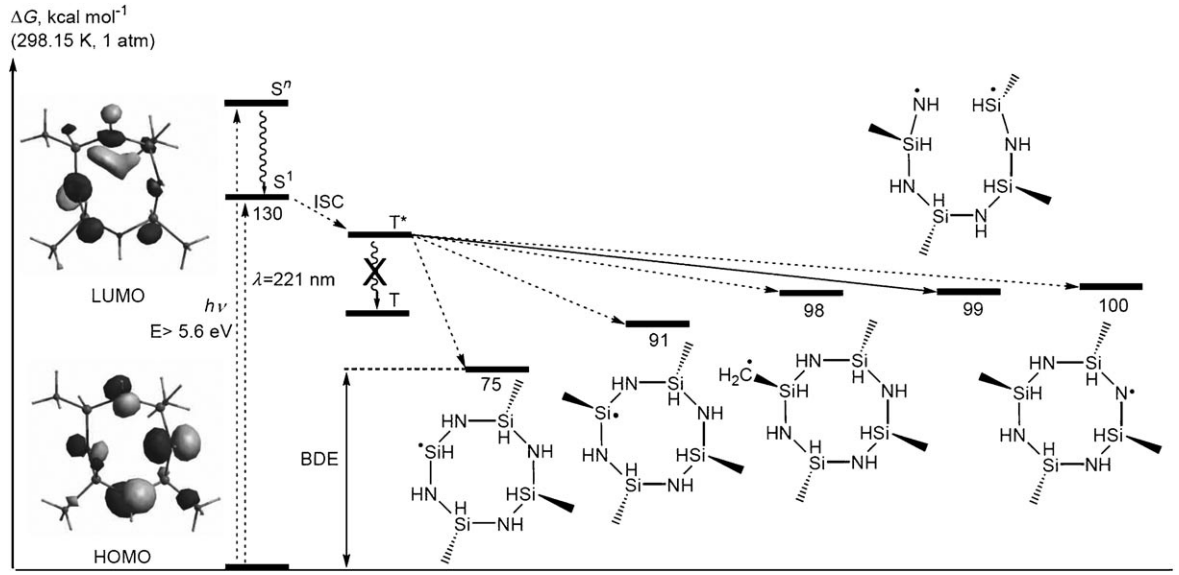

Figure 2. Quantum-chemical calculations on the photolytical excitation of TMCTSz and possible fragmentation pathways.

bonds of tetramethylcyclotetrasilazane were 100, 99, 98, 91, and 75 kcal mol^{-1}, respectively. Consequently, all types of bonds present in the molecule may be subject to dissociation. All dissociation reactions proceed exothermally with respect to the excited state. It should be noted that the smallest BDE was calculated for Si–CH_3 bond scission, which in fact takes place, as approved by gas phase IR measurements and by the kinetic investigations (vide infra). However, regardless of the higher BDE, Si–NH bond scission is expected to be the preferred reaction pathway, which can be rationalized by the favorable change of electron distribution from the Si–NH bond upon excitation (Figure 2, left side). By comparing the HOMO and LUMO orbitals (the latter can be taken as a first approximation of the electron distribution in the excited state), it is clear that excitation leads to a strong intramolecular electron shift from nitrogen to silicon, resulting into a reduced Coulomb attraction between these atoms, and therefore gives raise to a weakening of the corresponding –Si–NH– bond. Thus, the partial charges in the ground state of +0.80 e and −0.80 e at Si and N, respectively, change to +0.54 e (Si) and −0.35 e (N) in the excited state.

Similar calculations on perhydro- and octamethylcyclotetrasilazane revealed that the bond dissociation energies of the N–H, Si–NH, C–H, Si–H, and Si–CH_3 bonds shifted only by a few kcal mol^{-1}. The calculated BDEs for perhydro- and octamethylcyclotetrasilazane are given in the Supplementary Information (see the Supporting Information Table S1). Concomitantly, the absorption threshold of these compounds shifted towards lower energies and accounted for 5.8 eV (214 nm), 5.6 eV (221 nm), and 5.5 eV (227 nm) in the cases of perhydrocyclotetrasilazane, TMCTSz and octamethylcyclotetrasilazane, respectively. Accordingly, the oscillator strength grew distinctly and amounted to 0.045, 0.075, and 0.141, respectively, suggesting increasing absorption coefficients (vide infra). In summary, these calculations suggest that high energetic UV irradiation can in fact trigger the conversion of methylsilazanes into methyl-Si-O-Si networks. The reaction pathway may be based both on Si–NH bond scission followed by oxidation similar to PHPS,[7] and on the degradation of methyl groups (Si–C scission). However, as a result of the different absorption coefficients of the monomers in the ground state, irradiation with different wavelengths, that is, with 172, 185, or 222 nm, could in fact lead to different results with respect to reaction kinetics and depth profiles.

Transmission measurements and barrier properties of the coatings: Using synchrotron irradiation, the VUV/UVC transmission in the wavelength range $150 < \lambda < 240$ nm of P(DMS*co*MS) layers, 120 ± 10 nm in thickness and spin-coated onto quartz discs, was measured. It was found that the transmission spectra were very close to that of PHPS reported in ref. [21]. They were characterized by an absorption edge around 225 nm and a continuously decreasing transmission reaching a value of 0.18 at 165 nm. Additional UV/Vis transmission measurements on P(DMS*co*MS) dissolved in acetonitrile confirmed these absorption edges around 225 nm (Figure S02, Supporting Information). For example, the molar absorption coefficients of P(DMS*co*MS) at 230, 222, and 200 nm were 25, 78, and 920 dm^3 mol^{-1} cm^{-1}, respectively. Two conclusions can be drawn from these experiments. First, as suggested by quantum-chemical calculations, only irradiation with photons below 225 nm should be able to initiate photochemical reaction in these compounds. Second, the lower the chosen wavelength is the higher the absorption and, therefore, the lower the penetration depth of the UV light into layers of P(DMS*co*MS) will be. This calls for high-intensity irradiation sources. Aiming at the irradiation of square meter-sized areas for industrial applica-

tions, only a few intense radiation sources within this wavelength range are commercially available, that is, mercury low-pressure (HgLP) lamps that have a narrowband emission line at 185 nm, xenon excimer (XeExc) lamps that emit photons at 172 nm, and krypton/chlorine excimer (KrClExc) lamps with a narrowband emission at 222 nm.

TOF-SIMS and XPS measurements: Results of TOF-SIMS measurements on P(DMS*co*MS) layers irradiated with a 185 nm HgLP lamp in the presence of O_2 revealed both well expressed depth gradients of the relevant species C^-, SiN^-, and SiO_2^- and the influence of the irradiation time, respectively, the irradiation dose on their concentration (Figure 3).

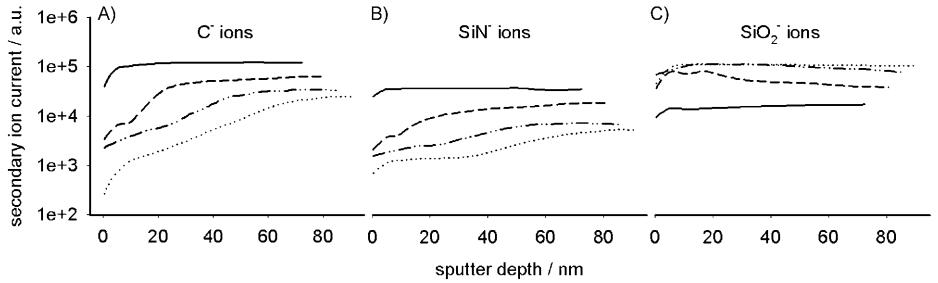

Figure 3. TOF-SIMS profiles of A) C^-, B) SiN^-, and C) SiO_2^- anions of P(DMS*co*MS) layers on silicon, untreated (——), irradiated by a HgLP lamp for 3 min (-----), 10 min (···-) and 30 min (•••••).

Decreasing values for C^- and SiN^- anions accounted for both an increased degradation of the methyl groups and the decomposition of the silazane backbone. An increase in SiO_2^- anions, however, verified the proceeding oxidative conversion of the starting compound, that is, P(DMS*co*MS). Obviously, the loss of carbon is a consequence of the release of C containing species from the layer, most probably as volatile compounds (vide infra). Comparative measurements on samples irradiated at wavelengths of about 172 nm, 185 nm, and 222 nm, respectively, revealed that shallower concentration gradients for the C^-, SiN^-, and SiO_2^- anions were observed with decreasing photon energy. Figure 4 gives an illustration of the C^- anion gradient within different P(DMS*co*MS) coatings along with the homogeneous profiles of an air-dried and a thermally treated sample of P(DMS*co*MS), respectively. As can be clearly seen, longer irradiation wavelengths coming along with lower absorption coefficients displayed increased penetration depths, leading to a more homogeneous energy deposition and concomitantly to a more homogeneous chemical conversion of the layer.

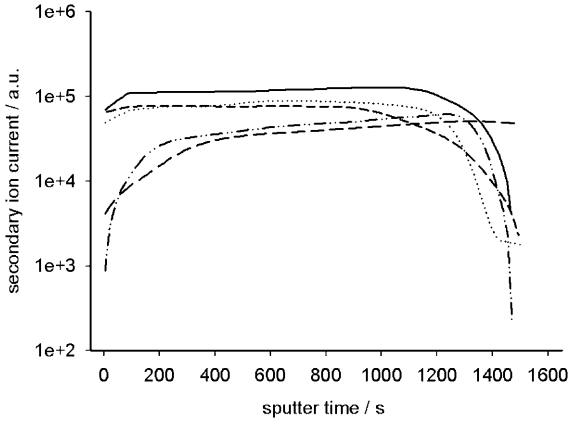

Figure 4. TOF-SIMS depth profiles of carbon concentration (C^- anions) in P(DMS*co*MS) layers: air-dried (——), thermally converted for 17 h at 200 °C (-----), and UV irradiated using 222 nm (•••••), 185 nm (– – –) and 172 nm (–·–) radiation.

In agreement with TOF-SIMS results, XPS measurements on P(DMS*co*MS) samples thermally cured for 17 h at 200 °C as well as UV cured by 172 nm and 222 nm photons, respectively, showed quite different element concentrations on the sample surface (Table 1). Thermal curing and curing by 222 nm irradiation, respectively, resulted in similar surface concentrations of C, O, and Si; these values were additionally very close to the theoretical ones of cured P(DMS*co*MS), suggesting that the methyl-Si–NH-Si network had quantitatively been transformed into a methyl-Si-O-Si one. However, in case of 172 nm irradiation, the surface concentration of C and O was completely different, that is, the carbon content decreased to one third in favor of the oxygen content indicating a more intensive degradation of the methyl functionalities. Disregarding potential dose rate effects, these findings can be attributed to the higher dose absorbed by the material close to the surface compared to the one absorbed from irradiations at longer wavelengths. High-resolution XPS measurements of the surface of similar samples supported this assumption. Thus, applying a peak fitting program to the C1s peak structure at a binding energy of about 285 eV, which is dominated by the carbon peak for saturated hydrocarbon (C–H) at 285.2 eV, a shoulder at 286.7 eV and a peak at 289.3 eV could be separated (Figure S2, Supporting Information). These peaks were assigned to C–O and O=C–O moieties.[26] For samples irradiated with 172 nm light, these peaks account for 10.3 and 9.0 %, respectively, of the overall C1s peak area. These findings point at the genera-

Table 1. Chemical composition of the surface of various P(DMS*co*MS) layers, as measured by XPS.

	C1s Peak [atom %]	O1s Peak [atom %]	Si2p Peak [atom %]	N1s Peak [atom %]
theoretical composition of cured P(DMS*co*MS)	36.3	36.3	27.3	0
thermal curing (24 h@ 200 °C)	33.3	39.1	25.5	2.2
irradiation@222 nm	35.7	37.8	25.4	1.1
irradiation@172 nm	11.3	59.8	26.6	2.4
quartz (SiO_2)	0	66.7	33.3	0

tion of Si–$CH_2^{\bullet}$ radicals formed by H-abstraction on the methyl group and subsequent oxidation of the carbon. For thermally cured as well as for 222 nm irradiated samples, the C–O shoulder was also detected; however, to a much lower extent accounting for 5.9% and 4.5%, respectively, of the C1s peak. The O=C–O peak was not observed at all. This clearly indicates that a decrease in irradiation wavelength results in an increase in Si–C degradation and thus underlines the necessity of choosing the appropriate irradiation source.

In many applications, the surface energy and especially the water contact angle of coated layers are of high practical interest, for example, peel strength or water vapor permeation. For thermally cured P(DMS*co*MS) layers (17 h, 200 °C), the surface energy amounted to 27 mN m^{-1} with disperse and polar fractions of 24 and 3 mN m^{-1}, respectively. The water contact angle was found to be 89°. Samples cured by 172 nm irradiation featured increased values accounting to 37 mN m^{-1} and 11 mN m^{-1} for the surface energy and for its polar fraction, respectively. This increase in surface energy was accompanied by a decrease in the water contact angles to about 70°. The according values obtained after 185 nm and 222 nm irradiation were close to those obtained by 172 nm irradiation (Table 2). Again, these results strongly support a VUV-triggered degradation of Si–C-bonds in the starting material and/or the final methyl-Si-O-Si layer.

Table 2. Water contact angles and surface energies of different P(DMS*co*MS) layers.

	Water contact angle [°]	Surface energy [mN m^{-1}]	Disperse fraction [mN m^{-1}]	Polar fraction [mN m^{-1}]
Thermally cured 17 h @ 200 °C	89	27.3	24.2	3.1
XeExc1, 14 J cm^{-2}	70	37.2	26.2	11.0
HgLP, 14 J cm^{-2}	72	35.6	25.1	10.5
KrClExc, 14 J cm^{-2}	66	39.7	26.4	13.3

Kinetic investigations: Using FTIR spectrometry in the transmission mode, kinetics of the decrease of the Si–H, the Si–CH_3 and the Si–NH–Si bands at 2170 cm^{-1}, 1270 cm^{-1} and 1180 cm^{-1}, and of the increase of the Si–O–Si band around 1050 cm^{-1} were studied on P(DMS*co*MS) layers spin-coated onto Si-wafers. Measurements were conducted at 172, 185, and 222 nm, respectively, using an oxygen concentration of 0.25 vol%. Because of the high absorption coefficient of oxygen for 172 nm light ($\alpha_{172nm} = 17$ cm^{-1}),[27] measurements at oxygen concentrations of 2.0 vol% were only carried out with 185 and 222 nm light, respectively. Details on measurement and the analyses are described elsewhere.[21]

The FTIR spectra, summarized in Figure 5, were recorded for a 100 nm P(DMS*co*MS) layer before and after irradiation by an HgLP lamp at $[O_2] = 0.25$ vol%. The kinetics of both the Si–CH_3 and Si–NH–Si degradation as well as of

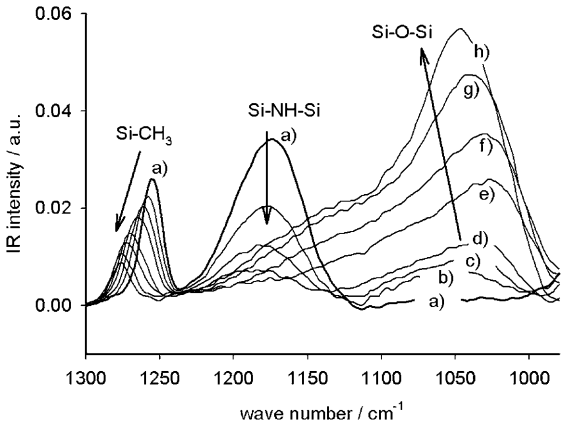

Figure 5. IR spectra in the wave number range between 980 and 1300 cm^{-1} of a 100 nm P(DMS*co*MS) layer before (a) and after irradiation with a HgLP lamp ($P_{VUV} = 12$ mW cm^{-2}, $[O_2] = 0.25$ vol%) for b) 1.5, c) 3, d) 6, e) 12, f) 24, g) 48, and h) 96 min.

the Si–O–Si formation were determined via integration of the areas of the corresponding vibration bands. Si–NH–Si degradation, which is indicative for Si–NH scission, was found to proceed fast apparently following first-order kinetics ($k_{app} = 6.8 \times 10^{-2}$ s^{-1} and $k_{app} = 4.9 \times 10^{-2}$ s^{-1} for 172 and 185 nm irradiation, respectively) at an irradiation dose rate of $P_{VUV} = 12$ mW cm^{-2}. These decomposition rates are slightly lower than the corresponding values found for PHPS which amounted to 8.2×10^{-2} s^{-1} and 5.8×10^{-2} s^{-1}.[21] In case of 222 nm irradiation, the rate constant was found to be 7.6×10^{-2} s^{-1}, however, at an almost 10 times higher dose rate of 100 mW cm^{-2}. For a meaningful comparison of the kinetic investigations one has to take into account that different absorption coefficients at different irradiation wavelengths determine the absorbed power, which in turn determines the rate constants. In earlier work on PHPS,[21] we already lined out that for 222 nm photons with an UV exposition power of 100 mW cm^{-2}, the power actually absorbed by a 100 nm layer was approximately the same as for 185 nm or 172 nm photons and an exposition power of 12 mW cm^{-2}, that is, about 10 mW cm^{-2}. By relating Si–NH–Si degradation in polyorganosilazanes to the dose actually absorbed by the layer and fitting the data to the exponential law $A = \exp(-k_D D_{VUV})$ (A = peak area, k_D = dose-related rate constant of Si–NH–Si decomposition, D_{VUV} = VUV dose absorbed by the layer), it was found that for all wavelengths used, the dose-related rate constants k_D were virtually the same and amounted to approximately 6×10^{-3} cm^2 mJ^{-1}. Thus, in the wavelength range $172 \leq \lambda \leq 222$ nm the kinetics of Si–NH–Si and Si–CH_3 decomposition are basically determined by the absorbed dose and not by the photon energy. Interestingly, k_D for P(DMS*co*MS) is almost 5 times higher than the corresponding value for PHPS (1.35×10^{-3} cm^2 mJ^{-1}).[21] This significant difference can not be explained by the inaccuracy of the calculated dose actually absorbed by the layer, which is in turn a result of the errors in the determination of the absorption coefficients and layer thickness (typically $\leq 20\%$). Instead, this difference is explained by the higher quantum

yields of photolytically initiated Si–NH bond scission as suggested by quantum-chemical calculations (vide supra).

The apparent rate constants of the $Si–CH_3$ degradation determined from the IR peak at 1270 cm^{-1} were in the range of 3×10^{-4} s^{-1} at dose rates of 12 $mW\,cm^{-2}$ for 185 nm and 100 $mW\,cm^{-2}$ for 222 nm, respectively. This approximately corresponds to a dose-related rate constant of 3×10^{-5} $cm^2\,mJ^{-1}$. A distinct dependence of the rate constants on the partial pressure of oxygen was observed.

The rate constants of the formation of Si–O–Si bands between 1030 and 1080 cm^{-1} showed an increase with increasing oxygen content. For 185 and 222 nm irradiation, an increase in the O_2-content from 0.25 to 2 vol% resulted in an increase in the rate constant from 8.3×10^{-4} s^{-1} to 1.8×10^{-3} s^{-1} and from 1.2×10^{-3} s^{-1} to 1.8×10^{-2} s^{-1}, respectively. These rate constants correspond to an increase in the dose-related constants of 8.3×10^{-5} $cm^2\,mJ^{-1}$ to 1.8×10^{-4} $cm^2\,mJ^{-1}$, and 1.2×10^{-4} s^{-1} to 1.8×10^{-3} $cm^2\,mJ^{-1}$, respectively.

Finally, as successfully accomplished for PHPS,[21] we aimed to accelerate the oxidative conversion of the Si–NH-Si network of P(DMS*co*MS) into the corresponding methyl-Si-O-Si network. For that purpose, basic catalysts, for example, dimethylethanolamine, diethylethanolamine, diazabicycloundecane, diazabicyclooctane and the Schwesinger base P_4-t-Oct, were tested. However, in contrast to PHPS, no significant acceleration in either the Si–NH–Si decrease or in Si-O-Si formation was observed with any of these catalysts. Similarly, no influence on the $Si–CH_3$ kinetics was observed.

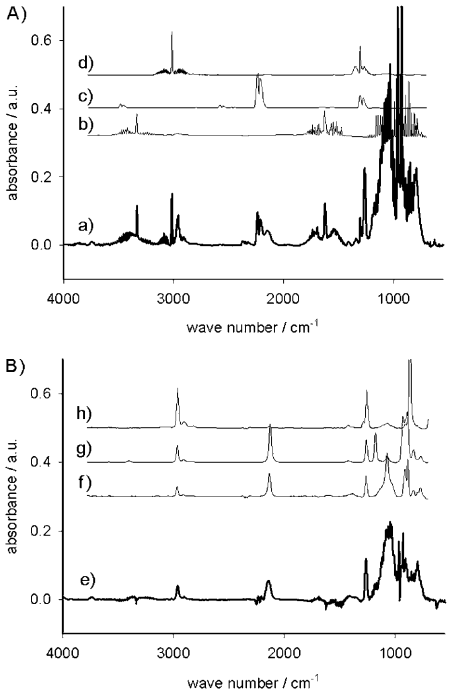

Figure 6. A, a) IR spectrum of the gas phase above a P(DMS*co*MS) layer after irradiation with a 222 nm lamp in a nitrogen atmosphere containing 1 vol.% oxygen, and IR spectra of b) ammonia, c) nitrous oxide, and d) methane. B, e) Difference spectrum derived from a) minus weighted curves b), c) and d), and the spectra of f) TMDSo, g) TMS, and h) TMDSz.

FTIR measurements of gaseous photolysis products: The irradiation-induced decrease of CH_3 and NH groups posed the question for the fate of these species. Figure 6 (top) shows the IR spectrum of the gas phase above a P(DMS*co*MS) layer on polyethylene terephthalate (PET) foil after irradiation with a 222 nm lamp in an oxygen-containing atmosphere (curve a). Beside of residual amounts of carbon dioxide and water vapor in the optical path of the spectrometer, ammonia with its characteristic bands at 930, 950, 1630, and 3420 cm^{-1} (curve b), nitrous oxide with a strong double band at 2268 and 2238 cm^{-1} (curve c), and methane with bands at 1306 cm^{-1} and 3015 cm^{-1} (curve d) could be identified (ref. [28] and own measurements). This is in accordance with findings reported by Han et al., where ammonia and methane were detected as the main volatile products in the pyrolysis of poly(methylsilazane)s at 870 °C in a nitrogen atmosphere.[29]

Irradiation at 222 nm of gaseous ammonia under the same conditions also resulted in the formation of N_2O. Hence, N_2O can be formed by means of photolytically-initiated oxidation of ammonia independent of the photolytic scission of the Si–NH bonds. Irradiation of ammonia with 185 nm and 172 nm photons from the HgLP lamp and the XeExc1 lamp, respectively, also yielded N_2O. However, irradiation of NH_3 with 254 nm photons from an HgLP lamp did not result in the formation of N_2O. These findings are in accordance with the absorption spectrum of ammonia, which is characterized by a series of Rydberg states with increased absorptions starting below 225 nm (absorption coefficient at 222 nm $\alpha_{222nm}=1$ cm^{-1}).[27,30] In case of methane, a further oxidation caused by photo-excitation was not observed. Having an absorption edge at 145 nm,[31] the absorption coefficient of methane for the wavelengths ranges of all the UV lamps used here was $<1\times10^{-4}$ cm^{-1} [27] and direct photolysis did therefore not occur.

Besides of considerable amounts of ammonia, nitrous oxide and methane, further bands were visible in the FTIR spectrum. Figure 6B shows the difference spectrum (curve e) of the IR spectrum (A, curve a) after weighted subtraction of the spectra of ammonia, nitrous oxide and methane. Curve f represents the spectrum of tetramethyldisiloxane (TMDSo, own measurements) with its characteristic peaks at 2960 and 2895 cm^{-1} (CH_3, CH_2), 2120 cm^{-1} (Si–H), and 1250 cm^{-1} ($Si–CH_3$). These bands show considerable agreement with the respective bands of the residual spectrum. However, the spectrum of various silanes also fit the observed spectrum well. For comparison, the spectrum of tetramethylsilane (TMS)[28] is shown in curve g. The weak shoulder at 1180 cm^{-1} (Si–NH–Si bonding) and the broad band at 870–970 cm^{-1} (Si–H, Si–N)[16] may indicate the presence of low molecular-weight silazanes. For comparison, the spectrum of tetramethyldisilazane (TMDSz, curve h, own measurement) is shown. The diffuse band around 3400 cm^{-1} may be assigned to the $\nu_{O–H}$ stretching vibration bands in silanols.[17] It can thus be assumed, though without any proof, that compounds connatural to TMDSo, TMS, and TMDSz

might be responsible for the remaining absorption bands after subtraction of ammonia, nitrous oxide and methane.

Finally, with reference to the congruent IR bands and within the respective detection limits, methanol, carbon monoxide, formaldehyde, formic acid, acetaldehyde, acetone, hydrogen cyanide, acetonitrile, ozone, methylamine, and other oxides of nitrogen beside of nitrous oxide could not be related to the gas phase FTIR spectra after irradiation of P(DMS*co*MS) under various conditions. By flushing the measurement chamber of the IR spectrometer with nitrogen it could be shown that carbon dioxide does not emerge in detectable amounts, as well.

Comparing the irradiation at different wavelengths (172, 185 or 222 nm) in the presence of oxygen (0.25 vol%), no significant differences were observed. However, owing to dose effects, the quantitative relations between methane, ammonia and nitrous oxide were found to be different. Irradiation in pure nitrogen containing traces of oxygen in the ppm range or irradiation in vacuum (1×10^{-4} mbar) resulted in spectra with reduced intensities of oxygen-containing species and also in lower concentration of ammonia. The latter must be a result of the higher proportion of recombination reactions inside the polysilazane network owing to the absence of other reaction partners, that is, oxygen. Finally, irradiation of the model compound 1,1,2,2-tetramethyldisilazane by 222 nm photons in the gas bulb in an N_2 atmosphere containing 1 vol.% of O_2 caused the decrease of the Si–NH–Si band at 1175 cm^{-1}. This process was accompanied by an increase of the Si–O–Si band around 1070 cm^{-1}. The Si–CH_3 band at 1260 cm^{-1} decreased only slightly. Ammonia, nitrous oxide and traces of methane could be detected. Additionally, in agreement with published work,[32] a fine white powder was deposited at the walls of the bulb.

In summary; i) the irradiation-induced conversion of the methyl-Si–NH-Si network of P(DMS*co*MS) into a methyl-Si-O-Si network, as well as the conversion of tetramethyldisilazane to tetramethyldisiloxane, is accompanied by the formation and release of ammonia and most probably its further oxidation to nitrous oxide, ii) the disappearance in the IR spectra of CH_3 groups can be explained by the release of methane after photoinitiated Si–CH_3 bond scission, followed by abstraction of a hydrogen atom from vicinal CH_3, SiH, or NH groups, iii) decomposition products, such as methane, support the involvement of both $H^{\bullet}$ and $CH_3^{\bullet}$ radicals.

P(DMScoMS)-derived O_2- and water vapor barrier layers: Finally, efforts were made to produce and characterize P(DMS*co*MS)-derived methyl-Si-O-Si layers for applications as barrier layers versus oxygen and water vapor. For this purpose, a roll-to-roll coating process was carried out applying slit-nozzle-coating on a coating machine at band speeds up to 10 m min^{-1}. 60–100 nm layers were applied to a 36 μm PET foil. The coating machine was equipped with IR dryers for evaporating the solvent (dibutyl ether, DBE) and with arrays of HgLP lamps and both types of XeExc lamps for generating 185 and 172 nm photons, respectively. In preliminary experiments it has been found that coatings made from pure P(DMS*co*MS) alone possess only inessential barrier properties against oxygen and water vapor. This is attributed to the presence of a considerable fraction of space-claiming methyl groups, which in turn decrease the number of cross-links within the network; the layers formed are less dense compared to those made from pure PHPS. After adding P(DMS*co*MS) (5 and 10 wt% with respect to PHPS) to a solution of PHPS (2 wt% in DBE), the oxygen transmission rate (OTR) and the water vapor transmission rate (WVTR) of machine-cured foils could be improved compared to a layer generated from pure PHPS by a factor of 2. Thus, an OTR of <1 $cm^3m^{-2}d^{-1}bar^{-1}$ and a WVTR of <4 $gm^{-2}d^{-1}$ for layers less than 100 nm thick were accomplished. Both the OTR and WVTR remained unchanged over at least three months. The water contact angles of these coatings were found to be around 35°.

Conclusions

Quantum-chemical calculations were performed on methyl substituted cyclotetrasilazanes, serving as model compounds. It was found that irradiation with VUV light at wavelengths <225 nm may initiate the oxidative conversion of the silazanes into partly methyl-substituted SiO_x networks. Transmission measurements on thin poly(1,1-dimethylsilazane-*co*-1-methylsilazane) (P(DMS*co*MS)) layers as well as UV/Vis measurements on dissolved P(DMS*co*MS) confirmed this finding. Using UV lamps with emission wavelengths of 172, 185, and 222 nm, respectively, thin P(DMS*co*MS) layers were irradiated and evaluated applying different techniques. Time-of-flight secondary ion mass spectroscopy (TOF-SIMS) and X-ray photo electron spectroscopy (XPS) measurements disclosed that the conversion process begins from the surface of the layer, which is most probably owed to the depth-dose profile of the penetrating irradiation. According to FTIR measurements, the decomposition rate of the Si–NH-Si network was found to be close to that for PHPS and turned out to be basically independent of the wavelength of the UV light. The kinetics of the degradation of the methyl substituents also did not depend on the irradiation wavelength. This is in agreement with quantum-chemical calculations. Compared to the photolytically induced decomposition processes, the formation of the methyl-Si-O-Si network was slower and is dependent on the oxygen concentration. For all these processes, kinetic data were determined at various irradiation wavelengths and oxygen concentrations. Addition of a base as a catalyst did not significantly accelerate the oxidation process.

FTIR measurements in the gas phase above the irradiated P(DMS*co*MS) revealed the presence of ammonia and methane as main products, as well as nitrous oxide, which is presumably formed from ammonia. Gas barriers were prepared from 60–100 nm coatings based in both perhydropolysilazane (PHPS) and P(DMS*co*MS) applying a roll-to-roll process at band speeds up to 10 m min^{-1}. Long-term stable barrier layers with OTR and WVTR values of

$<1\,cm^3\,m^{-2}\,d^{-1}\,bar^{-1}$ and $<4\,g\,m^{-2}\,d^{-1}$, respectively, were obtained. This process was accompanied by an increase in hydrophilicity. To investigate the mechanism of the VUV-initiated conversion of P(DMS*co*MS) in more detail, EPR, and NMR measurements as well as GC-MS analyses are in progress and will be reported in due course.

Experimental Section

P(DMS*co*MS) and P(MS*co*MVS) (trade names HTA 1500 and HTT 1800, respectively) were obtained from Clariant Produkte GmbH (Sulzbach, Germany). 1,1,3,3-Tetramethyldisilazane (TMDSz), tetramethylsilane (TMS), and 1,1,3,3-tetramethyldisiloxane (TMDSo) were purchased from ABCR (Karlsruhe, Germany). *n*Butyl acetate (for analysis), dibutyl ether (for synthesis) and acetonitrile were purchased from Merck KGa (Darmstadt, Germany). Aqueous ammonia solution (25 wt% NH_3) was obtained from Riedel-de Haen (Seelze, Germany). Methane gas was from Messer Griesheim (Düsseldorf, Germany). As catalysts for the acceleration of the oxidative conversion process the following compounds were tested: 2-(dimethylamino)ethanol (DMEA), 2-(diethylamino)ethanol (DEEA), 1,8-diazabicyclo[5.4.0]undec-7-ene (DBU), are all from Merck (Darmstadt, Germany), 1,4-diazabicyclo[2.2.2]octane (DABCO), and the Schwesinger base 1-tert-octyl-4,4,4-tris(dimethylamino)-2,2-bis-[tris(dimethylamino)phosphoranylidenamino]-2Λ5,4Λ5-catenadi(phosphazene) (P4-t-Oct), both from Fluka (Taufkirchen, Germany). UV/Vis spectra were measured on the scanning spectrophotometer UV-2101 PC (Shimadzu, Kyoto, Japan).

The conversion of P(DMS*co*MS) into methyl-Si-O-Si networks was studied using FTIR in transmission mode. These experiments were conducted on spin-coated 2 inch silicon wafers (Si-Mat, Landsberg/Lech, Germany). For spin-coating, 10 and 20 wt% solutions, respectively, of P(DMS*co*MS) in *n*butyl acetate were prepared, optionally, appropriate amounts of catalyst were added. To obtain layers of the desired thickness of about 100 nm the spin-coating conditions were the following: acceleration at $300\,rpm\,s^{-1}$ to a speed of 3000–5000 rpm, held for 1 min. To obtain a nearly solvent-free layer, the coated wafers were stored at ambient temperature in air for about 30 min. FTIR measurements were performed on an IFS55 instrument (Bruker GmbH, Karlsruhe, Germany).

Gas phase IR measurements were carried out using a bulb consisting of a high-purity quartz tube (Suprasil, Heraeus Noblelight, Kleinostheim), 60 mm in diameter, 200 mm in length, equipped with NaCl windows at the front sides (diameter 60 mm, thickness 5 mm). The bulb was equipped with two vacuum-tight valves for purging and a septum screw as an injection window on the shell. Pieces of PET foils $7\times18\,cm^2$, 36 μm in thickness, were dip-coated on one side with polysilazane solution, dried in air for 10 min, and then inserted into the cell. The application weight of the air-dried coating was determined gravimetrically. For P(DMS*co*MS) layers it was found to be in the range of $20\,g\,m^{-2}$. The bulb was evacuated to a pressure less than 1×10^{-4} mbar using a vacuum pumping station consisting of a membrane pump and a turbomolecular pump (Pfeiffer Vakuum GmbH, Asslar, Germany) in order to remove oxygen to a maximum extent. Then, the bulb was flushed for 10 min with nitrogen or with a mixture of 99 vol% nitrogen and 1 vol% oxygen (both from Air Products, Hattingen, Germany). The loaded bulb was irradiated for 5 min using either XeExc1, XeExc2, HgLP or KrClExc UV lamps (vide infra). Additionally, these irradiation experiments were carried out on unloaded bulbs and on bulbs loaded with uncoated PET foils to ensure the absence of contaminations and of products originating from sources other than the P(DMS*co*MS)-based layers. After the treatments described above, the gas volume of the bulbs was analyzed by FTIR. To avoid erroneous interpretation of the CO_2 band, the measuring chamber of the spectrometer was purged with nitrogen for 10 min before each measurement. The resulting spectra were evaluated using the OPUS/SEARCH 5.5 software package from Bruker and the NIST/EPA Gas Phase Infrared Library.

Four different types of UV lamps were used as sources for irradiation experiments: a Xe_2* excimer lamp[24] 172/630 Z (XeExc1) with an emission at $\lambda=172\pm12$ nm, maximum VUV intensity $30\,mW\,cm^{-2}$; a KrCl* excimer lamp 222/300 (KrClExc) with a narrowband emission at $\lambda=222\pm1.2$ nm and a maximum UVC intensity of $25\,mW\,cm^{-2}$. Both lamps were purchased from Heraeus Noblelight (Kleinostheim, Germany). In addition, a Xe_2* excimer lamp XERADEX 20 L40/120 (XeExc2) (Radium Lampenwerk Wipperfürth, Germany), $\lambda=172\pm12$ nm, VUV power $12\,mW\,cm^{-2}$, and an array of mercury low-pressure lamps UVI80 US 15/395 (HgLP, uv-technik Speziallampen GmbH, Wümbach, Germany), with relevant emission lines at $\lambda=184.9$ and 253.7 nm and with an VUV intensity of $12\,mW\,cm^{-2}$ for the first line were used. Irradiations were performed in a chamber flushed with N_2 containing defined concentrations of O_2 (50 vppm to 20.6 vol%). The distance between the (V)UV lamps and the sample surface was 26 mm. The technical gases used came from Air Products (Hattingen, Germany). Depth profiles of TOF-SIMS spectra were recorded on a TOF-SIMS V system (ION-TOF GmbH, Münster, Germany). Details are described elsewhere.[21]

The chemical composition on the sample surface was determined using a SAGE 100 XPS spectrometer from specs (Berlin, Germany). Surfaces were cleaned with an Ar ion beam for 10 min prior to analysis. High resolution XPS measurements were carried out on a PHI 5000 Versa Probe Scanning X-ray Microprobe (Physical Electronics GmbH, Ismaning, Germany).

Roll-to-roll coating experiments were carried out using a laboratory coating machine from EHA Spezial-Maschinenbau GmbH (Steffenberg, Germany) for band widths up to 500 mm equipped with a 200 mm wide slit-nozzle from Coatema Coating Machinery GmbH (Dormagen, Germany) for application of the coating solution, and with carbon-IR dryers 1000 W (Heraeus Noblelight, Germany) and arrays of XeExc1, XeExc2 and HgLP UV lamps (vide supra). The slit nozzle was fed by a gear pump Reglo-Z Digital ISM 901 from Ismatec GmbH (Wertheim-Mondfeld, Germany). PET foils (Lumirror 40.01, 36 μm in thickness, 200 mm in width) were obtained from Pütz GmbH&Co. Folien KG (Taunusstein, Germany). Surface energies were determined using a G2 contact angle measuring system from Krüss (Hamburg, Germany) by measuring and evaluating the contact angles of water and diiodomethane on the sample surface. Synchrotron measurements were carried out at the BESSY synchrotron (Physikalisch-Technische Bundesanstalt, Berlin, Germany).

Acknowledgements

These studies have been supported by the Bundesministerium für Bildung und Forschung, BMBF, contract no. 01RI06007, the Federal State of Germany and the Free State of Saxony. The authors are grateful to Thomas Groß und Dr. Andrey Lyapin from Physical Electronics GmbH, Ismaning, as well as Dr. Stefan Zürcher from SuSoS AG, Dübendorf, for high resolution XPS measurements and especially for the analysis of the data on the C1s peak.

[1] H. Chatham, *Surf. Coat. Technol.* **1996**, *78*, 1.
[2] J. Madocks, J. Rewhinkle, L. Barton, *Mater. Sci. Eng. B* **2005**, *119*, 268.
[3] Y. Leterrier, *Prog. Mater. Sci.* **2003**, *48*, 1.
[4] F. Kessler, D. Herrmann, M. Powalla, *Thin Solid Films* **2005**, *480*, 491.
[5] D. Pech, P. Steyer, A. S. Loir, J. C. Sanchez-Lopez, J. P. Millet, *Surf. Coat. Technol.* **2006**, *201*, 347.
[6] T. N. Chen, D. S. Wuu, C. C. Wu, C. C. Chiang, Y. P. Chen, R. H. Horng, *J. Electrochem. Soc.* **2006**, *153*, F244.
[7] J. Fricke, H. Schwab, U. Heinemann, *Int. J. Thermophys.* **2006**, *27*, 1123.
[8] F. Fracassi, R. d'Agostino, F. Palumbo, E. Angelini, S. Grassini, F. Rosalbino, *Surf. Coat. Technol.* **2003**, *174–175*, 107.

[9] E. Angelini, S. Grassini, F. Rosalbino, F. Fracassi, S. Laera, F. Palumbo, *Surf. Interface Anal.* **2006**, *38*, 248.
[10] K. Reichelt, X. Jiang, *Thin Solid Films* **1990**, *191*, 91.
[11] A. Gruniger, P. R. von Rohr, *Thin Solid Films* **2004**, *459*, 308.
[12] A. G. Erlat, B. C. Wang, R. J. Spontak, Y. Tropsha, K. D. Mar, D. B. Montgomery, E. A. Vogler, *J. Mater. Res.* **1999**, *15*, 704.
[13] S. Iwamori, Y. Gotoh, K. Moorthi, *Surf. Coat. Technol.* **2003**, *166*, 24.
[14] T. P. Chou, C. Chandrasekaran, G. Z. Cao, *J. Sol-Gel Sci. Technol.* **2003**, *26*, 321.
[15] H. Kriegsmann, G. Engelhardt, *Z. Anorg. Allg. Chem.* **1961**, *310*, 100.
[16] K. Kamiya, T. Tange, T. Hashimoto, H. Nasu, Y. Shimizu, *Res. Rep. Fac. Eng. Mie Univ.* **2001**, *26*, 23.
[17] T. Kubo, E. Tadaoka, H. Kozuka, *J. Sol-Gel Sci. Technol.* **2004**, *31*, 257.
[18] F. Bauer, U. Decker, A. Dierdorf, H. Ernst, R. Heller, H. Liebe, R. Mehnert, *Prog. Org. Coat.* **2005**, *53*, 183.
[19] C. Kato, S. Tanaka, Y. Naganuma, T. Shindo, *J. Photopolym. Sci. Technol.* **2003**, *16*, 163.
[20] Y. Naganuma, S. Tanaka, C. Kato, T. Shindo, *J. Ceram. Soc. Jpn.* **2004**, *112*, 599.
[21] L. Prager, A. Dierdorf, H. Liebe, S. Naumov, S. Stojanović, R. Heller, L. Wennrich, M. R. Buchmeiser, *Chem. Eur. J.* **2007**, *13*, 8522.
[22] EP0745974B1, JP11092666AA, JP10279362AA.
[23] Y. Leterrier, Y. Wyser, J. A.e. Manson, *J. Adhes. Sci. Technol.* **2001**, *15*, 841.
[24] B. Eliasson, U. Kogelschatz, *Appl. Phys. B* **1988**, *46*, 299.
[25] Gaussian 03, Revision B.02, M. J. Frisch, G. W. Trucks, H. B. Schlegel, G.e. Scuseria, M. A. Robb, J. R. Cheeseman, V. G. Zakrzewski, J. A. J. Montgomery, R.e. Stratmann, J. C. Burant, S. Dapprich, J. M. Millam, A. D. Daniels, K. N. Kudin, M. C. Strain, O. Farkas, i. J. Tomas, V. Barone, M. Cossi, R. Cammi, B. Mennucci, C. Pomelli, C. Adamo, S. Clifford, J. Ochterski, G. A. Petersson, P. Y. Ayala, Q. Cui, K. Morokuma, P. Salvador, J. J. Dannenberg, D. K. Malick, A. D. Rabuck, K. Raghavachari, J. B. Foresman, J. Cioslowski, J. V. Ortiz, A. G. Baboul, B. B. Stefanov, G. Liu, A. Liashenko, P. Piskorz, I. Komaromi, R. Gomperts, R. L. Martin, D. J. Fox, T. Keith, M. A. Al-Laham, C. Y. Peng, A. Nanayakkara, M. Challacombe, P. M. W. Gill, B. Johnson, W. Chen, M. W. Wong, J. L. Andres, C. Gonzalez, M. Head-Gordon, E. S. Replogle, J. A. Pople, Gaussian, Inc., Pittsburgh, **2003**.
[26] G. Beamson, D. Briggs, *High Resolution XPS of Organic Polymers. The Scienta ESCA300 Database*, Wiley, New York, **1992**.
[27] B. A. Thompson, P. Harteck, R. R. Reeves, *J. Geophys. Res.* **1963**, *68*, 6431.
[28] NIST, National Institute of Standards and Technology (NIST) **2005**.
[29] H. N. Han, D. A. Lindquist, J. S. Haggerty, D. Seyferth, *Chem. Mater.* **1992**, *4*, 705.
[30] M. Suto, L. C. Lee, *J. Chem. Phys.* **1983**, *78*, 4515.
[31] F. Z. Chen, C. Y. R. Wu, *J. Quant. Spectrosc. Radiat. Transfer J. Quant. Spectrosc. Ra.* **2004**, *85*, 195.
[32] J. Pola, A. Galikova, Z. Bastl, J. Subrt, K. Vacek, J. Brus, A. Ouchi, *Appl. Organomet. Chem.* **2006**, *20*, 648.

Received: August 11, 2008
Published online: November 28, 2008

